Statistics of Single-Electron Signals in Electron-Multiplying Charge-Coupled Devices

Taras Plakhotnik, Arjun Chennu, and Andrei V. Zvyagin

***Abstract*—Electron-multiplying charge coupled devices promise to revolutionize ultrasensitive optical imaging. The authors present a simple methodology allowing reliable measurement of camera characteristics and statistics of single-electron events, compare the measurements to a simple theoretical model, and report camera performance in a truly photon-counting regime that eliminates the excess noise related to fluctuations of the multiplication gain.**

***Index Terms*—Charge coupled device (CCD), low-light level imaging, noise, photon counting, single-photon detection.**

I. Introduction

AN ELECTRON-MULTIPLYING charge coupled device (EMCCD) is an advanced imaging device that contains an additional multiplication register creating a multielectron charge package for every primary electron via an impact-ionization cascade [1]. As a result, the relative contribution of the readout noise is reduced dramatically [2], [3]. Such cameras are most valuable for ultrasensitive imaging (including single-molecule microscopy and detection). Ultimately, sensitivity is hindered by various sources of noise, and analysis of noise in an EMCCD at the single-photon detection level is the major subject of this paper.

Since electron multiplication is a statistical process, it generates extra noise in EMCCD images (excess noise), which should be taken into account when estimating the ultimate sensitivity of EMCCD cameras. Thermally generated electrons are common both for the ordinary CCD and for the EMCCD and can be substantially reduced by cooling the EMCCD sensor down to 200 K or even lower. Clock-induced charges (CICs) or spurious charges generated in the process of electron multiplication are EMCCD specific and can make a significant addition to the resulting signal at low light intensities [4], [5]. Because the electron multiplication gain is sensitive to temperature and suffers from aging, a precise calibration of camera output versus image brightness presents a problem. An effective usage of EMCCD cameras relies on adequate understanding of all these factors.

In this paper, we present a simple analytical model for the distribution of single-photonlike events in EMCCDs and demonstrate its validity experimentally. This model leads to a new and simple methodology allowing reliable measurement of the electron multiplication factor, the thermal electron, and the CIC contributions. Also, we analyze an EMCCD operation in a truly photon-counting regime, which reveals the possibility to eliminate the excess noise associated with the statistical fluctuations of the multiplication gain.

Manuscript received October 26, 2005; revised January 10, 2006. The review of this paper was arranged by Editor J. Hynecek.

T. Plakhotnik and A. Chennu are with the School of Physical Sciences, University of Queensland, Brisbane, Qld 4072, Australia (e-mail: taras@physics.uq.edu.au).

A. V. Zvyagin is with the School of Physical Sciences and the School of Information Technology and Electrical Engineering, University of Queensland, Brisbane, Qld 4072, Australia.

Digital Object Identifier 10.1109/TED.2006.870572

II. Theoretical Description of a Noise in EMCCD

Multistage multiplication in the EMCCD multiplication register can be considered as a process where the probability of multiplication of every electron is a constant independent on the stage [3], [6]. Such multiplication creates an electron avalanche, which has been simulated numerically using a Monte Carlo approach [3] or a probability-generating function [6]. However, a simple analytical description is much more convenient for the purpose of the experimental data analysis. Suitable theoretical frameworks have been derived to describe avalanche processes in gas discharge and in nuclear-physics detectors [7], [8]. It has been shown that the probability to obtain n electrons out of one primary electron after M-stage electron multiplication (with the average multiplication gain per stage equal to $1+\alpha$) is

$$P(n) = \frac{1}{\bar{G}} \exp\left(-\frac{n}{\bar{G}}\right) \tag{1}$$

where $\bar{G}$ is the average gain factor $\bar{G} = (1+\alpha)^M$. This equation is valid if $\bar{G} \gg 1$ and therefore n can be treated as a continuous variable. When the probability p_p for obtaining one electron (primary generated charge) per pixel is much smaller than 1, the distribution of the readout signals from camera pixels is given by $(1-p_p)\delta(n) + p_p \bar{G}^{-1} \exp(-n/\bar{G})$, where the δ function describes the output signal when a pixel has no primary electron. This distribution function should be convoluted with a Gaussian distribution describing the additive noise produced in the charge-to-voltage conversion process. An average electronic dc offset n_0 is usually present in the camera output and should be taken into account. If the Gaussian distribution width is much smaller than the width of the exponential distribution given by (1), the resulting distribution can be approximated by the following expression

$$P(n) = \frac{1-p_p}{\sigma\sqrt{2\pi}} \exp\left(-\frac{(n-n_0)^2}{2\sigma^2}\right) + \frac{p_p}{\bar{G}} \exp\left(\frac{n_0-n}{\bar{G}}\right) \theta(n-n_0) \tag{2}$$

where $\theta(x)$ is a step function [$\theta(x) = 0$, if $x < 0$, and $\theta(x) = 1$, if $x \geq 0$] and where p_p depends on the illumination intensity and the exposure time for the photoelectron-related part as well as the sensor temperature and the integration time for thermal electrons. In addition to an electron-multiplying register, an EMCCD camera has an ordinary electronic circuit converting a charge to a digital output. We then treat $\bar{G}$ as a cumulative gain, which includes the charge-to-count conversion factor, and consider n as a digitized output (stored in the computer memory). Note that the precise value of the cumulative gain factor is required for assessing the number of photoelectrons generated in the sensor.

The distribution of the output signal related to the CIC does not obey (1) because spurious electrons are created in the multiplication register and therefore do not follow the same path as primary thermal electrons and photoelectrons. To take this factor into account, we generalize (2) by assuming the following multiexponential distribution of the pixel outputs at a low illumination level:

$$P(n) = \frac{p_z}{\sigma\sqrt{2\pi}} \exp\left(-\frac{(n-n_0)^2}{2\sigma^2}\right) + \left[\frac{p_p}{\bar{G}} \exp\left(\frac{n_0-n}{\bar{G}}\right) + p_c \sum_{k=1}^{k_{\max}} \frac{A_k}{\bar{G}_k} \exp\left(\frac{n_0-n}{\bar{G}_k}\right)\right] \theta(n-n_0) \quad (3)$$

where we introduced the probability p_c of having a CIC at the output and $p_z \equiv 1 - p_c - p_p$ for briefness. We neglect the probability that a CIC and a primary generated charge can contribute to the same pixel output (that is, $p_p, p_c \ll 1$). Parameters A_k are assumed to be normalized, $\sum A_k = 1$. To separate different factors contributing to (3), the following methodology has been developed. We first acquired L frames, numbered them, and then subtracted every odd frame from the preceding even frame. The $L/2$-long sequence of such differenced frames has been used to obtain a histogram of readout differences. This histogram was calculated by counting number of pixels with a given value of n in the differenced frames. As a result, an offset free symmetrical histogram (that is dependent on $|n|$) was obtained. The theoretical description for this histogram is

$$H(n) = \left[\frac{p_z - p_p - p_c}{2\sigma\sqrt{\pi}} \exp\left(-\frac{n^2}{4\sigma^2}\right) + \frac{p_p}{\bar{G}} \exp\left(-\frac{|n|}{\bar{G}}\right) + p_c \sum_{k=1}^{k_{\max}} \frac{A_k}{\bar{G}_k} \exp\left(-\frac{|n|}{\bar{G}_k}\right)\right] N_x \quad (4)$$

where N_x is the total number of pixels in one frame. The dispersion of the Gaussian part is $2^{1/2}$ times larger in (4) than in (3), because the readout noises from two frames add up when the differenced frame is calculated. At the same time, the number of pixels containing primary or clock-induced electrons doubles. During our measurements, we have noticed that the offset n_0 may exhibit a small drift with a characteristic time on the order of 10 s. This affects the experimental data and makes the comparison with theory more difficult. Therefore n_0-independent (4) is a convenient basis for the data analysis.

For example, to extract the contribution from photoelectrons, two such histograms should be measured for different exposure times and/or mean illumination intensities. Assuming that CIC and thermal electrons are not affected by these variations [4], the theoretically expected difference $\Delta H(n)$ between these two histograms is

$$\Delta H(n) = \left[\frac{\Delta p_p}{\bar{G}} \exp\left(-\frac{|n|}{\bar{G}}\right) - \frac{\Delta p_p}{\sigma\sqrt{\pi}} \exp\left(-\frac{n^2}{4\sigma^2}\right)\right] N_x \quad (5)$$

where Δp_p is the change of p_p due to the change of the number of the photoelectrons.

III. Experimental Details and Results

To verify the validity of (5), an EMCCD (Andor Ixon, 512 × 512 pixel camera, 16×16 μm^2 pixel size) was illuminated with a light emitting diode (LED) powered by a pulse generator with a variable duty cycle. The pulse generator was synchronized with the EMCCD readout cycle; therefore, by changing only the duty cycle of the pulse generator, it was possible to vary precisely the total number of photoelectrons accumulated by the sensor of the EMCCD before the readout. In the experiment, the duty cycles were selected as 20, 40, 60, and 80%. The total number of photons incident on the sensor during the integration time varied in proportion of 1:2:3:4, respectively. The sensor was uniformly illuminated and a set of neutral density optical filters was used to reduce the intensity of the illumination to a very low level (when the probability to generate one primary photoelectron in a camera pixel was much lower than 1). The EMCCD camera was operated in a "kinetic mode" to record consecutive frames with a minimum delay between them. The readout rate was set to 1 MHz in most experiments. To reduce the effect of CIC, the vertical shift speed was increased by setting the corresponding clock time to 0.4 μs. To eliminate CIC and thermal-electron contributions from the four histograms (corresponding to the four duty cycles of the LED), a reference histogram measured with the LED switched OFF was subtracted from each of the four. Similarly, kinetic series were acquired when the sensor was kept dark and with the exposure times set to 0.1 (reference) and 10 s. This allowed us to study the effects of the thermally generated electrons. Results of these measurements are presented in Figs. 1 and 2. Both figures demonstrate excellent agreement with (5). Fig. 1 also displays an excellent linearity (the total number of detected photo counts varies as 1:1.99:2.98:3.91, which should be compared to the 1:2:3:4 variation of the duty cycle) expected for low illumination intensities. More importantly, these results yield the total number of photoelectrons detected on average by the EMCCD in a single frame. These numbers (which are equal to $\Delta p_p N_x$, where Δp_p can be found by fitting (5) to experimental data) were obtained without *a priori* knowledge of the cumulative gain factor $\bar{G}$. Because the multiplication gain strongly depends on the sensor temperature and is affected by aging, the use of (5) provides the most accurate measurement of absolute light intensities due to immunity to the multiplication gain and/or charge-to-count factor variations. The thermal electron generation rate (see Fig. 2) is very low and can be neglected in

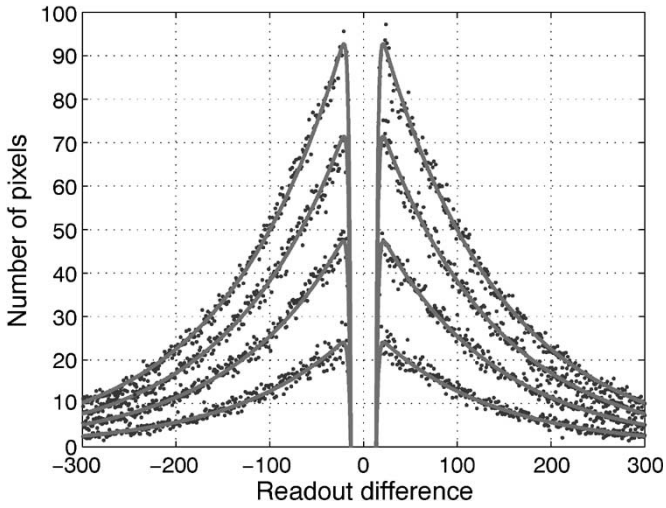

Fig. 1. Linearity test and exponential distribution of the multiplication factors for single-electron per pixel inputs. The EMCCD camera was operated at 1-MHz readout rate, −70-°C temperature, and 0.4-μs shift speed. Dots are experimental points and solid lines correspond to the theoretical dependence given by (5). There are three parameters for each curve. The most probable values for integrals under exponents (that is $\Delta p_p N_x$) as defined by the least-square criteria are equal to 3554 ± 40, 7076 ± 47, 10 601 ± 54, and 13 905 ± 60. The cumulative gain factor $\bar{G}$ is 122.6, 124.4, 124.0, and 125.6, respectively. The standard deviation σ of the readout noise is 4.0, 3.9, 3.9, and 3.4 (from bottom to the top).

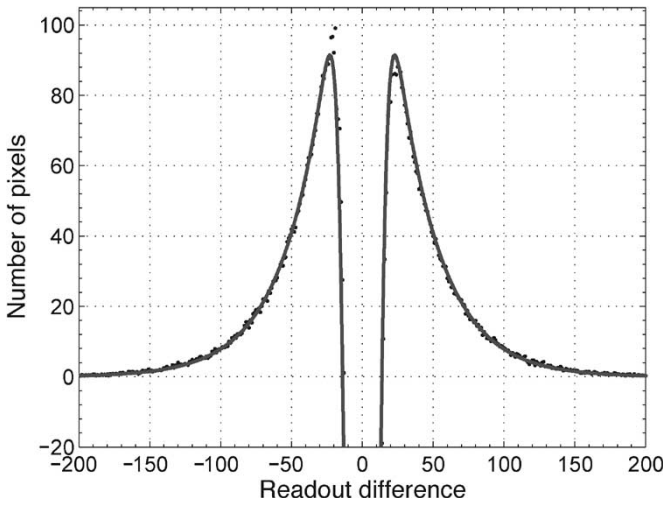

Fig. 2. Dark count rate measurements. The differenced image histograms were measured with the camera shutter closed and for two exposure times (0.1 and 10 s), and the dots represent the difference between the two histograms. The EMCCD camera was operated at 5-MHz readout rate, −70-°C temperature, and 0.4-μs shift speed. The total number of thermally generated electrons is 6453 per 9.9 s, equivalent to 0.0025 counts/s/pixel.

comparison to the CIC, provided the exposure time is shorter than 10 s and the sensor temperature is not elevated (see next section).

IV. CIC and Photon Counting

To study CIC, a histogram was measured under conditions when the contributions from photo and thermal electrons were minimal (closed camera shutter and a short exposure time). Equation (4) was used to fit an experimental histogram shown in Fig. 3. From the results presented in Fig. 2, one can estimate

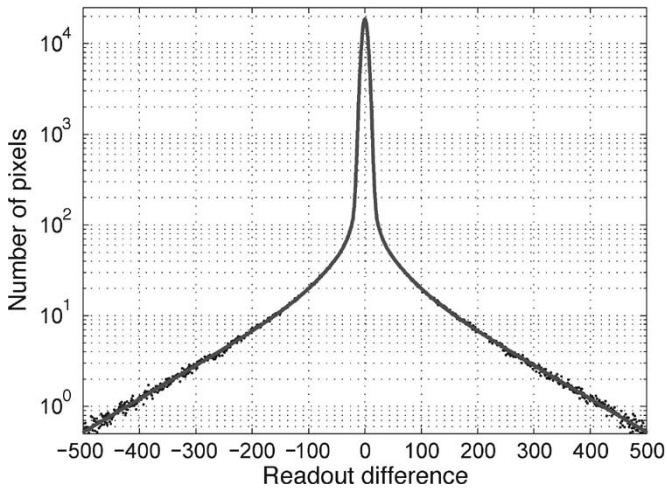

Fig. 3. CIC distribution. Camera settings: readout of 1 MHz, sensor temperature of −70 °C, and accumulation time of 0.1 s. The data (dots) were fitted (solid line) using one Gaussian and three exponential functions [see (4)]. Fitting parameters: $\sigma = 3.7$, $G_1 = 120$, $A_1 = 0.36$, $A_2 = 0.24$, $G_2 = 35$, $A_3 = 0.40$, $G_3 = 7.8$, and $p_c = 0.045$ counts/pixel/frame.

that $p_p \approx 2.5 \times 10^{-4}$ for the conditions described in the figure caption of Fig. 3. For simplicity, we set $p_p = 0$ and treat Fig. 3 as representing a histogram for a pure CIC signal. It turned out that only three exponents ($k_{\max} = 3$) were sufficient to describe the experimental results accurately. The fitting parameters are given in the figure caption. Note that the slowest decaying exponent (the highest average gain) in Fig. 3 is very close to the exponent describing the distribution of the multiplication factors for photo and thermal electrons (see Figs. 1 and 2). This is not totally surprising because $\bar{G}$ is the highest possible electron gain in the system. A large weight factor of the high gain exponent (indicating that a substantial amount of CICs is primarily created close to the beginning of the multiplication register) is valuable information. However, the applicability of the three exponent approximation for EMCCDs of different manufacturers needs verification. Although principles of operation of all EMCCDs are identical, some differences may result from variations in the designs.

To simplify the analysis of the signal-to-noise ratio (SNR), we will assume that $\bar{G} = G_1$. It is important to note that, based on this approximation, the multiplication gain can be obtained without a light source but by analyzing the CIC-signal distribution.

For the analysis of the SNR, we return to (3), integrate $\int_0^\infty nP(n)dn$, and multiply it by N_x to get a mean value $\bar{S}$ of the signal in one frame. The result is

$$\bar{S} = N_x \left[n_0 + p_p \bar{G}_1 + p_c \sum_{k=1}^{3} A_k \bar{G}_k \right] \tag{6}$$

of which the variance $\sigma_{\bar{S}}^2$ is

$$\sigma_{\bar{S}}^2 = N_x \left[p_z \sigma^2 + 2p_p \bar{G}_1^2 + 2p_c \sum_{k=1}^{3} A_k \bar{G}_k^2 \right]. \tag{7}$$

The SNR in this case is calculated according to $\mathrm{SNR}_{\mathrm{int}} = (\bar{S} - \bar{S}_0)/(\sigma_{\bar{S}}^2 + \sigma_{\bar{S}_0}^2)^{1/2}$, where $\bar{S}_0$ and $\sigma_{\bar{S}_0}^2$ are the values given by (6) and (7) in the absence of photoelectrons (that is when $p_p = 0$, since we neglect thermal electrons for simplicity). The SNR characterizes the difference between frames with and without a signal. We did not attempt image recognition. The SNR defined above explicitly reads as

$$\mathrm{SNR}_{\mathrm{int}} = \frac{N_x^{\frac{1}{2}} p_p}{\left((2 - 2p_c - p_p)\frac{\sigma^2}{\bar{G}_1^2} + 4p_c \sum_{k=1}^{3} A_k \frac{\bar{G}_k^2}{\bar{G}_1^2} + 2p_p\right)^{\frac{1}{2}}}. \tag{8}$$

If the Gaussian noise and the CIC are negligible, the $\mathrm{SNR}_{\mathrm{int}} = (N_x p_p/2)^{1/2}$ and is $2^{1/2}$ times smaller than the theoretical limit determined by the square root of the average number of detected photons, that is, $(N_x p_p)^{1/2}$. The excess noise factor of $2^{1/2}$, due to the fluctuations of the multiplication gain inherently present in an EMCCD, agrees with results published in literature [3], [9]–[11]. One can attempt to suppress this noise by counting only pixels of which the signal satisfies the condition $n - n_0 \geq n_t$. This approach is analogous to the photon-counting technique widely used in, for example, photomultiplier tube-based sensors. Integrating the probability density (3) over the region $n - n_0 \geq n_t$, we obtain the probability for getting a pixel above the threshold P_t as

$$P_t = p_c \sum_{k=1}^{3} A_k \exp\left(-\frac{n_t}{\bar{G}_k}\right) + p_p \exp\left(-\frac{n_t}{\bar{G}_1}\right) + \frac{1 - p_p - p_c}{\sigma\sqrt{2\pi}} \int_{n_t}^{\infty} \exp\left(-\frac{n^2}{2\sigma^2}\right) dn. \tag{9}$$

The mean number of pixels having $n - n_0 \geq n_t$ is $\bar{N}_{\mathrm{cnt}} = N_x P_t$ and its variance (given by the binominal distribution) is $\sigma_{\mathrm{cnt}}^2 = N_x P_t (1 - P_t)$. The SNR is defined in analogy with $\mathrm{SNR}_{\mathrm{int}}$ as $\mathrm{SNR}_{\mathrm{cnt}} \equiv (\bar{N}_{\mathrm{cnt}} - \bar{N}_{cnt,p_p=0})/(\sigma_{\mathrm{cnt}}^2 + \sigma_{cnt,p_p=0}^2)^{1/2}$. For example, by taking the limit $\sigma \to 0$ (neglecting Gaussian noise) and setting $n_t \approx 0$, the SNR simplifies to

$$\mathrm{SNR}_{\mathrm{cnt}} \approx \frac{N_x^{\frac{1}{2}} p_p}{(2p_c + p_p)^{\frac{1}{2}}}. \tag{10}$$

The corresponding noise-improvement factor is defined by

$$\frac{\mathrm{SNR}_{\mathrm{cnt}}}{\mathrm{SNR}_{\mathrm{int}}} \approx \left(\frac{4p_c A_1 + 2p_p}{2p_c + p_p}\right)^{\frac{1}{2}} \tag{11}$$

where the estimation is valid when, in addition to all other approximations, $G_1^2 \gg G_k^2, k \neq 1$ (which is the case for the camera under study). If A_1 equals 1, the improvement factor is $2^{1/2}$, independent of the values of p_c and p_p. But for $A_1 < 1$, the improvement factor is smaller. It can be even smaller than 1 (noise increases) for $p_p \ll p_c$. The exact optimization of n_t can be done numerically by using (9), the aforementioned expressions for $\bar{N}_{\mathrm{cnt}}$ and σ_{cnt}^2, and the definition for $\mathrm{SNR}_{\mathrm{cnt}}$. Fig. 4 presents the dependence of the noise-improvement factor on the average number of photo electrons (that is on $p_p N_x$, where we take $N_x = 512 \times 512$) for the choice of n_t, which provides the largest possible value of $\mathrm{SNR}_{\mathrm{cnt}}$ (note that generally such n_t depends on p_p) when the camera parameters ($\{A_k\}$, $\{\bar{G}_k\}$, σ, and p_c) are taken from Fig. 3. The results show that photon counting gives an advantage of up to 30% (if compared to simple integration). When $p_p > 0.1$, the probability of two photoelectrons generated per pixel is larger than 5% (assuming Poisson distribution), and the photon-counting algorithm shows the onset of saturation because of counting two photons as one.

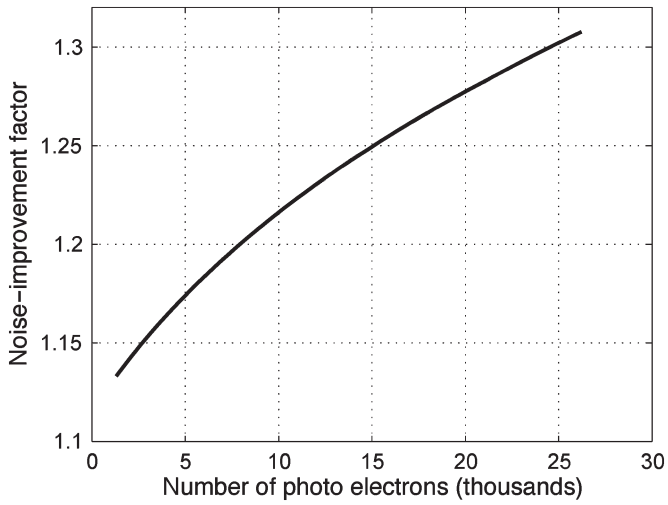

Fig. 4. Theoretical noise-improvement factor calculated for the parameters determined from Fig. 3.

V. Conclusion

We have presented a comprehensive theoretical model of the noise characteristics of EMCCD sensors. It has been shown that the distribution of the multiplication gain for photo and thermal electrons is in excellent agreement with a theoretical model considering history-independent multiplication on every stage and predicting an exponential distribution of the gain factors. The distribution of CICs or spurious charges is shown to be multiexponential. True photon counting based on imposing a threshold on the acquired image can be used to improve the SNR by a factor of up to $2^{1/2}$, but the statistics of CIC-related noise reduces the noise-improvement factor. However, in an experimentally useful range of photon numbers, the single-photon-counting procedure is still advantageous (the exact SNR improvement depends on the illumination level and the CIC-noise statistics). The proposed and demonstrated methodology of statistical analysis provides a simple way for obtaining absolute numbers of detected photons and true gain factors.

References

[1] S. K. Madan, B. Bhaumnik, and J. M. Vasi, "Experimental observation of avalanche multiplication in charge coupled devices," *IEEE Trans. Electron Devices*, vol. ED-30, no. 6, pp. 694–699, Jun. 1983.

[2] P. Jerram *et al.*, "The LLLCCD: Low light imaging without the need for an intensifier," *Proc. SPIE*, vol. 4306, pp. 178–186, 2001.

[3] M. S. Robbins and B. J. Hadwen, "The noise performance of electron multiplying charge-coupled devices," *IEEE Trans. Electron Devices*, vol. 50, no. 5, pp. 1227–1232, May 2003.

[4] O. Daigle, J.-L. Gach, C. Guillaume, C. Carignan, P. Balard, and O. Boisin. (2004). "L3CCD results in pure photon counting mode," in *Proc. SPIE—Int. Society Optical Engineering*, Glasgow, Scotland, vol. 5499, pp. 219–227. [Online]. Available: http://xxx.lanl.gov/ftp/astro-ph/papers/0407/0407315.pdf

[5] D. J. Denvir and E. Conroy, "Electron multiplying CCD technology: The new ICCD," in *Proc. SPIE—Int. Society Optical Engineering*, Seattle, WA, 2003, vol. 4796, pp. 164–174.

[6] J. Hynecek and T. Nishiwaki, "Excess noise and other important characteristics of low light level imaging using charge multiplying CCDs," *IEEE Trans. Electron Devices*, vol. 50, no. 1, pp. 239–245, Jan. 2003.

[7] R. A. Wijsman, "Breakdown probability of a low pressure gas discharge," *Phys. Rev.*, vol. 75, no. 5, pp. 833–838, Mar. 1949.

[8] G. D. Alkhazov, "Statistics of electron avalanches and ultimate resolution of proportional counters," *Nucl. Instrum. Methods*, vol. 89, no. 1, pp. 155–165, 1970.

[9] K. Matsuo, M. C. Teich, and B. E. A. Saleh, "Noise properties and time response of the staircase avalanche photodiode," *IEEE Trans. Electron Devices*, vol. ED-32, no. 12, pp. 2615–2623, Dec. 1985.

[10] J. N. Hollenhorst, "A theory of multiplication noise," *IEEE Trans. Electron Devices*, vol. 37, no. 3, pp. 781–788, Mar. 1990.

[11] J. Hynecek and T. Nishiwaki, "Recent progress toward single photon detection using charge multiplying CCD image sensors," in *Proc. 16th World Multiconf. Systems and Cybernetics*, Orlando, FL, Jul. 2002, pp. 7–12. no. 2.

Taras Plakhotnik received the M.S. degree from Moscow Physical Technical Institute, Moscow, Russia, and the Ph.D. degree from the Institute of Spectroscopy, Russian Academy of Sciences, Moscow, in 1982 and 1992, respectively.

After 1982, he started his scientific career as a Junior Researcher at the Institute of Spectroscopy, Russian Academy of Sciences. From 1993 to 1997, he simultaneously held research positions at the Institute of Spectroscopy and at the Swiss Federal Institute of Technology (ETH), Zurich, Switzerland. Later, he was a Habilitatnd and a Senior Research Assistant at ETH. Since 2004, he has been lecturing on physics and electronics at the University of Queensland, Brisbane, Qld, Australia. His expertise is on laser design, high-resolution spectroscopy, hole-burning technique, supersonic free-jet spectroscopy, intracavity laser spectroscopy, and statistics. His current research interest includes single-molecule detection, spectroscopy, and microscopy, a technique where he was one of the pioneers. He is the author or coauthor of more than 50 peer-reviewed journal publications.

Arjun Chennu was born in India in 1985. He is currently working toward the Bachelor of Technology degree in engineering physics at the Indian Institute of Technology, Madras, India.

His scientific interest is in condensed-matter physics, specifically in biophysics, photonics, and lasers.

Andrei V. Zvyagin was born in Russia on November 4, 1961. He received the Diploma from the Moscow Engineering Physics Institute, Moscow, Russia, in 1984 and the Ph.D. degree in engineering from Tokyo Institute of Technology, Tokyo, Japan, in 1997.

From 1984 to 1994, he spanned a range of positions from an Engineer to Senior Research Scientist in the Institute of Metrology for Time and Space, Moscow, Russia, focusing on research and metrological aspects of time and frequency standards based on trapped ions. From 1998 to 2000, he was a Postdoctoral Fellow in the Optical+Biomedical Engineering Laboratory, Department of Electrical, Electronic, and Computer Engineering, The University of Western Australia, Crawley, WA, Australia. From 2000 to 2004, became an Australian Postdoctoral Fellow, studying optical coherence tomography for biomedical imaging applications. From 2004 to 2005, he joined the Center for Biophotonics and Laser Science at the University of Queensland, Brisbane, Qld, Australia, as a Lecturer/Australian Research Fellow and was promoted to a Senior Lecturer/Australian Research Fellow since 2006. His research interest covers various areas of biophotonics and biomedical engineering, including optical scanning near-field microscopy, optical coherence tomography, optical coherence-domain imaging, fiber-optic spectroscopy for biological assaying *in vivo*, photoreceptor optics for vision research, and biological imaging assisted by novel molecular labels.